

Suspended Particle Characterization Using Convolution Neural Networks from Acoustic Backscatter Data

Joseph Hartley^{1, a)}, Lee Mortimer^{1, b)}, Jeffrey Peakall^{2, c)}, Richard Bourne^{1, d)},
Jonathan Dodds^{3, e)}, Michael Fairweather^{1, f)}, Timothy Hunter^{1, g)}

¹*School of Chemical and Process Engineering, University of Leeds, Leeds, LS2 9JT, United Kingdom*

²*School of Earth and Environment, University of Leeds, Leeds, LS2 9JT, United Kingdom*

³*National Nuclear Laboratory, Workington, Cumbria, CA14 3YQ, United Kingdom*

^{a)} *Corresponding author: pmjha@leeds.ac.uk*

^{b)} *l.f.mortimer@leeds.ac.uk*

^{c)} *j.peakall@leeds.ac.uk*

^{d)} *r.a.bourne@leeds.ac.uk*

^{e)} *jonathan.m.dodds@uknnl.com*

^{f)} *m.fairweather@leeds.ac.uk*

^{g)} *t.n.hunter@leeds.ac.uk*

Abstract. Artificial neural networks (ANNs) and convolution neural networks (CNNs) have been developed and demonstrated to simultaneously predict the particle mean diameter and concentration using ultrasonic backscatter data considering spherical silica glass beads suspended in a calibration tank. Training data was obtained across a range of concentrations (2.4 – 70.6 g.L⁻¹) and particle sizes (35.2 – 208 μ m) using the Metflow UVP-DUO instrumentation, measured at two transducer probe frequencies, 2 and 4 MHz. A preprocessor transforms the raw signal data into a normalized G-function for each measurement, which is used to train the ANN and CNN. The ANN performs well on the training dataset below around 250 epochs obtaining a mean square error of around 0.05, beyond which overfitting is observed. Upon switching to the CNN, a further improvement down to 0.04 is obtained and only 150 epochs are required to train the algorithm to this degree of accuracy. Overall, the CNN learns the features of the G-function data faster, and provides more accurate predictions of the particle properties demonstrating that patterns in the G-function play an important role in its relation to characterization. The presented results offer promise for the use of machine learning algorithms to process and analyze ultrasonic backscatter data, and serve as a foundation for more improved techniques in the future.

INTRODUCTION

Ultrasonic (US) backscatter (BS) has shown its ability to characterize a range of suspensions and slurries in industrial applications, specifically nuclear decommissioning, for many years as it allows non-contacting in situ characterization [1] [2]. Concentration profiles [3] and particle size [4] can be determined in bulk suspensions, and in pipe-flows US BS can be utilized for velocimetry, flow regime identification and concentration verification [2]. A limitation of the existing US analytical technique is the requirement to know either the concentration or particle size to determine the other. Machine learning (ML) offers the opportunity to bypass this since it can be defined as “algorithms that process and extract information from data, such that they facilitate automation of tasks and augment human domain knowledge” [5], allowing both to be determined simultaneously. This would prove extremely beneficial in nuclear applications as it would permit monitoring of such parameters in dynamic systems where both vary significantly [6].

Previously, ML has been used with US for identification of various processes [7] and characterization of US properties, detailed at length in the review by [8]. ML has also been used to characterize both suspension concentration and particle size, but with artificially generated BS data close to the probe face [9]. The work presented here expands on previous studies by utilizing US BS data gathered directly from well mixed suspensions rather than idealized data generated artificially and is directly comparable to studies using the same suspended material and existing US analytical techniques [3]. The use of CNNs rather than ANNs also offers an advancement to ML for this application. This study aims to demonstrate the applicability of ANNs and CNNs for determining key suspension parameters; concentration, average particle size and a measure of particle size distribution (PSD), from US BS data of homogeneous suspensions. Though driven by the needs of nuclear decommissioning, this advancement is applicable

to any industry with a need to determine suspension parameters of dynamic systems with non-contacting and/or in situ characterization methods.

METHODOLOGY

Ultrasonic backscatter data was gathered using a Metflow UVP-DUO with 2 and 4 MHz transducer probes submerged in a well-mixed calibration tank, to ensure a homogeneous sampling region. Nine systems of suspended spherical silica glass beads were measured at six concentrations; 2.4, 14.1, 26.2, 42.4, 56.5, and 70.6 gL⁻¹. These systems were made from individual monodisperse glasses; small, medium, and large, with d50 values of 35.2, 83.8, and 208 μm, respectively, as well as 25:75, 50:50, and 75:25 wt.% mixes of the small to medium, and medium to large monodisperse glasses. A Malvern Mastersizer 3000 was used to determine a PSD for each system, the d50 value and coefficient of variation were calculated, and with concentration, were used as labels for each backscatter profile. Raw backscatter data were averaged and the G-function method [3] was used to determine constants, which allow the existing analytical method to characterize suspensions of the same media where concentration is unknown, but an average size and/or PSD is known. The G-function method rearranges the backscatter voltage equation from the Thorne model [10] and takes the natural logarithm, as in Eq. (1). By taking two partial derivatives with respect to distance and concentration, the measured concentration independent sediment attenuation coefficient can also be determined from Eq. (2), which is used as a calibration for determining unknown concentrations of the same suspension system.

$$G = \ln(\psi r V) = \ln(k_t k_s) + \frac{1}{2} \ln M - 2r(\alpha_w + \alpha_s) \quad (1)$$

$$\xi^m = -\frac{1}{2} \frac{\partial}{\partial M} \left[\frac{\partial}{\partial r} [\ln(\psi r V)] \right] = -\frac{1}{2} \frac{\partial^2 G}{\partial M \partial r} \quad (2)$$

The concentration of each system was measured with three 2 MHz probes and two 4 MHz probes for a total dataset of 270 profiles. Upon obtaining the G-functions for each set of measurements, the data undergoes a pre-processing routine which consists of four parts. Firstly, the G-function data is cut, with noise present at either end of the backscatter penetration depth range removed to ensure only the central section remains. Secondly, the data is normalized, ensuring all data points are positive and reside within the range $G_N(r) \in [0,1]$. Thirdly, the data is interpolated onto 999 equally distributed points, ensuring that for a given raw input, the size of the input feature vector remains consistent. Finally, the probe frequency (2 MHz or 4 MHz) is appended to the end of the feature vector, acting as a single additional input, undergoing normalization equivalently to the G-function data and bringing the total input feature vector size to 1000. This pre-processing technique further allows for generalizability to a given ultrasonic backscatter measurement.

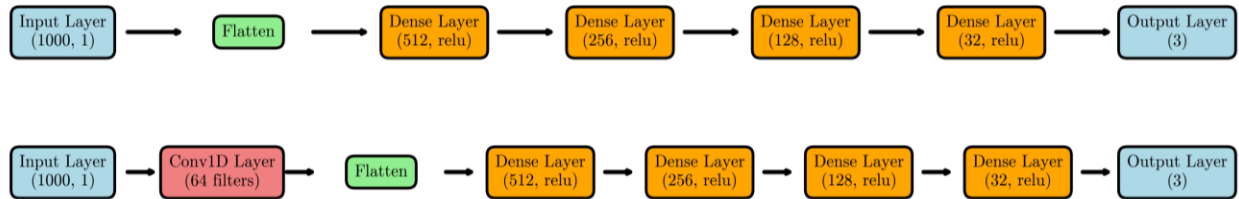


FIGURE 1. Description of ANN (upper) and CNN (lower) architecture. Brackets indicate either number of neurons alongside the activation function used, or in the case of the convolution layer, the number of filters.

Two neural network architectures were developed in order to predict the PSD and concentration for each G-function. A layer-wise description of these is present in Fig. 1. The ANN uses four hidden layers, reducing the number of neurons as the network becomes deeper. Each neuron uses the rectified linear unit (ReLU) activation function, and the final output layer consists of three neurons, corresponding to the normalized mean particle diameter, coefficient of variation on the distribution, and concentration. In the case of the CNN, there is an additional one-dimensional convolution layer which learns 64 filters, each of window size 10, and applies them to the input data to extract features. The aim of this additional layer is to extract features from sequential data which in the present case is the normalized

G-functional signal. Each filter slides along the input data sequence and performs an element-wise multiplication with the overlapping input values, summing up to produce a single output. This is repeated over the entire G-function signal, generating a feature map which is propagated through the further layers. Next, the flatten layer reshapes the output of the convolution layer into a one-dimensional tensor, which is propagated through the remainder of the network identically to the ANN technique. The ANN and CNN are both trained over 500 epochs, using the adam optimizer to minimize the mean absolute error which is used as the loss function. Each epoch uses a batch size of 32, and a train-test split of 0.3 for validation.

RESULTS AND DISCUSSION

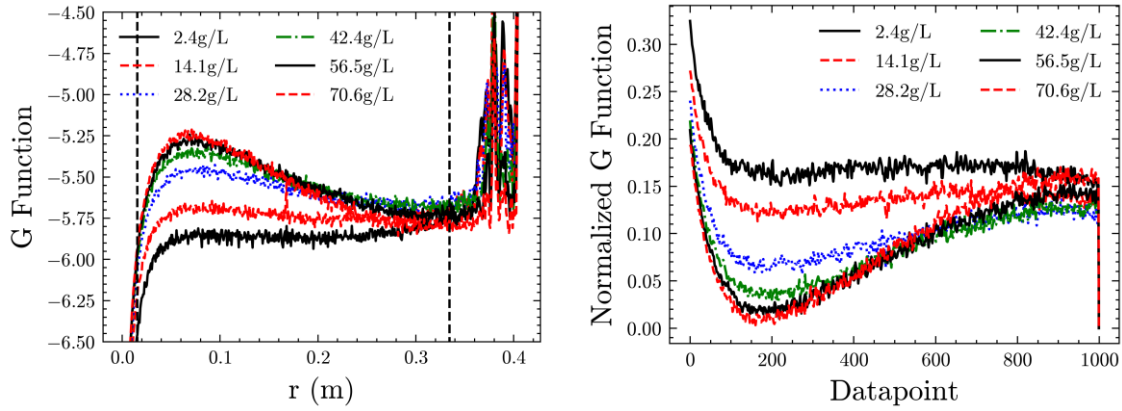


FIGURE 2. G-function (left) and normalized G-function (right) of the medium sized glass suspension for all concentrations tested from one 2 MHz probe.

An example of a full concentration range of the medium sized glass system is shown in Fig. 2, as G-function against distance from the transducer probe face, and the normalized G-function after pre-processing against datapoint number. In the G-function plot the vertical dashed lines correspond with where the 2 MHz data were cut to remove the noise, close to the probe face and from the bottom of the calibration tank. The initial crest relates to the near-field region of the acoustic wave where BS relationships are not linear as the acoustic wave propagates non-spherically. The region after the crest relates to the far-field region where attenuation is linear and is modeled by the Thorne model, as shown in Eq. (1). The position of the crest appears to vary depending on concentration, average particle size, and frequency so not all of it was cut. The tail end was cut simply to disregard the reflections and noise from the bottom of the calibration tank, thus as much of the profile as possible has been kept. The normalized G-function clearly keeps the positive mirrored shape of the original G-function and highlights the final normalized frequency as a final data point.

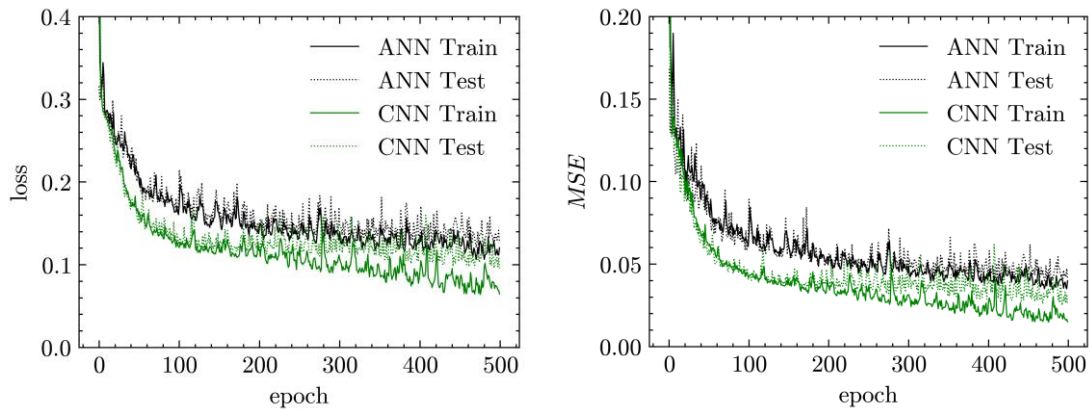


FIGURE 3. Evolution of loss function (left) and mean square error (MSE) (right) for training of both ANN (black) and CNN (green). Comparison of training data (solid line) and testing data (dashed line) is also presented.

The performance of both the ANN and CNN approaches are illustrated in Fig. 3. The evolution of the loss function with the training epoch is presented in the left plot. Both models begin with relatively high loss values, which decrease as the ANN and CNN learn, with the CNN dropping more sharply initially. The CNN shows consistently lower training and testing loss compared with the ANN, which indicates that the CNN is capable of learning patterns in the data more effectively. In the case of the ANN, overfitting is present beyond around 250 epochs, evidenced by the gap in the training and testing curves, and reaches a minimum loss before overfitting of around 0.15. The CNN generally performs better, though overfitting occurs earlier, at around 210 epochs, though the loss is reduced compared to the ANN, settling around 0.12 before overfitting. It is also of note that there is generally less noise present in the testing loss curve compared to that of the ANN, suggesting that the CNN is more suitable for reflecting accurate results for data it has not seen before. Similar observations can be made for the mean square error, with the CNN reaching greater accuracy faster, suggesting that the CNN is more efficient at capturing the relevant features from the G-function data.

CONCLUSIONS AND FURTHER WORK

The present study has considered the development, and demonstrated the effectiveness, of ANNs and CNNs in simultaneously predicting the particle size distribution and concentration from ultrasonic backscatter data. Labelled data from measurements performed on silica glass beads in homogeneous suspensions across a range of concentrations and particle sizes was obtained through multi-frequency ultrasonic probe experiments and used as training data. A pre-processing framework was designed and implemented to generalize the process to further real-world measurements, and normalized G-functions were used as input feature vectors, along with the corresponding probe frequency. The results indicate that while both techniques were capable of performing characterization, the CNN was shown to outperform the ANN both in terms of accuracy and efficiency. It is demonstrated that the CNN achieves a lower mean square error with fewer training epochs, likely due to its ability to predict patterns in the G-function sequential data more effectively. The presented findings highlight the potential of CNNs to enhance present analytical techniques, providing a strong foundation for further advancements in ML-informed characterization.

Further work should consider real-world application in nuclear decommissioning, acting as an in situ technique capable of determining the important characteristics of suspended particle-laden fluids, such as the size distribution and concentration. Alongside increasing the amount of training data through further experiments, the CNN scheme itself should also be extended to incorporate regularization techniques as well as further hyper parameter tuning in order to improve its performance.

ACKNOWLEDGMENTS

The authors are grateful to the UK Engineering and Physical Sciences Research Council for funding through the TRANSCEND (Transformative Science and Engineering for Nuclear Decommissioning) project (EP/S01019X/1), and Sellafield Ltd. for funding from the University of Leeds-Sellafield Ltd, Centre of Expertise for Sludge (Particulates & Fluids).

REFERENCES

1. T. N. Hunter, L. Darlison, J. Peakall and S. Biggs, *Chem. Eng. Sci.* **80**, 409-418 (2012).
2. S. T. Hussain, J. Peakall, M. Barnes and T. Hunter, *Proc. Mtgs. Acoust.* **45**, 070002 (2021).
3. A. S. Tonge, J. Peakall, D. M. J. Cowell, S. Freear, M. Barnes and T. N. Hunter, *Appl. Acoust.* **180**, 108100 (2021).
4. A. Vergne, C. Berni, J. Le Coz and F. Tencé, *Water Resour. Res.* **57**, e2021WR029589 (2021).
5. S. L. Brunton, B. R. Noack and P. Koumoutsakos, *Ann. Rev. Fluid Mech.* **52**, 477-508 (2020).
6. T. N. Hunter, J. Peakall and S. Biggs, *Miner. Eng.* **28**, 20-27 (2012).
7. A. L. Bowler, S. Bakalis and N. J. Watson, *Sensors* **20**, 1813 (2020).
8. A. L. Bowler, M. P. Pound and N. J. Watson, *Ultrasonics* **124**, 106776 (2022).
9. A. L. Gower, R. M. Gower, J. Deakin, W. J. Parnell and I. D. Abrahams, *Europhys. Lett.* **122**, 54001 (2018).
10. P. D. Thorne and D. M. Hanes, *Cont. Shelf Res.* **22**, 603-632 (2002).